Journal of the European Ceramic Society **18** (1998) 2339–2343
© 1999 Elsevier Science Limited
Printed in Great Britain. All rights reserved
PII: S0955-2219(98)00240-4
0955-2219/99/$—see front matter

Features of Corrosion Resistance of AlN–SiC Ceramics in Air Up to 1600°C

V. A. Lavrenko,[a]* M. Desmaison-Brut,[b] A. D. Panasyuk[a] and J. Desmaison[b]

[a]Institute for Problems of Materials Science, 3 Krzhyzhanovsky str., 2521 42 Kiev, Ukraine
[b]LMCTS, ESA CNRS 6015, Université de Limoges, 123, Avenue Albert Thomas, 87060 Limoges Cedex, France

Abstract

The kinetics and mechanism of (80% AlN + 20% SiC) and (50% AlN + 50% SiC) powders and ceramics oxidation in air up to 1600°C were studied with the aid of TG, DTA, XRD, EPMA, SEM and metallographic analysis methods. The ceramics samples were obtained by hot pressing fine-dispersion AlN and SiC powders with an average particle size of 1 μm at 1800°C for 2 h. This ensures a fine-grain material structure with a uniform distribution of phase components. It was shown that in a non-isothermal regime, a three-stage oxidation mechanism takes place. It was established that the scale formed consists of three oxide layers. In the inner layer, $Al_{10}N_8O_2$ *oxynitride and* β-SiO_2 *(cristobalite) phases were observed; in the intermediate layer, β-SiAlON was found for samples with a relatively low SiC content whereas* α-Al_2O_3 *was present in samples with a greater SiC content. The outer layer contains* $3Al_2O_3.2SiO_2$ *(mullite) as a main phase, the latter ensuring highly protective properties of the scale. The materials investigated can be considered as having extremely high resistance to corrosion up to 1550°C. © 1999 Elsevier Science Limited. All rights reserved*

1 Introduction

The AlN-SiC ceramics, obtained by powder metallurgy methods, have a high level of physicomechanical properties, i.e. high hardness, strength, wear- and corrosion-resistance at high temperatures. These properties make the materials attractive for application in different fields of contemporary technology.

There are literature data reporting extremely high corrosion resistance of SiC.[1,2] It has been established[1,3] that in the early stages oxidation and at lower temperatures, amorphous SiO_2 is the oxidation product, while for longer exposures, there is a tendency for SiO_2 crystallization (the β-cristobalite form). In the papers concerning high-temperature oxidation of pure AlN,[4-6] it has been shown that oxygen diffusion through a scale is the limiting step and an amorphous Al_2O_3 is an oxidation product at temperatures below 1100°C while α-Al_2O_3 forms above 1100°C.

High-temperature oxidation of ceramics in the SiC-AlN solid solution field was investigated by Y. Xu *et al.* [7] in air at 1370°C for 200 h. These authors showed that a 38 mass% SiC–62 mass% AlN material obtained by hot pressing at 2100°C for 1 h, has an oxidation rate constant which is two orders of magnitude higher than that of pure SiC. Herein a two-layer scale forms. In the inner layer, there are β-sialon and graphite; the outer layer contains mullite as a main phase. The goal of this work is to study oxidation in air both of powders and compact composite materials in the AlN-SiC system with SiC contents of 20 and 50 mass% as well as to define the oxidation mechanism and interaction products for different temperature up to 1550°C.

2 Experimental Procedure

The compact 80% AlN–20% SiC and 50% AlN–50% SiC samples were obtained by hot pressing fine-dispersion powder mixtures (the average size of particles was 1 μm) at 1800°C for 2 h. This leads to materials with a very fine structure and a uniform distribution of phase components.

Oxidation of powders and hot-pressed solid ceramics was investigated in air by TG and DTA methods up to 1550°C in a nonisothermal regime with a sample heat rate of 15°C/min and also in the isothermal condition at 1350°C for 225 min using a Setaram apparatus. The phase composition of interaction products at different temperatures was studied by XRD and chemical analysis methods. The structure and element distributions in the scale were defined using cross sections perpendicular to

---

*To whom corespondence should be addressed.

the sample surfaces by means of EPMA and SEM methods using a Camebax MS46 apparatus.

3 Results and Discussion

Using TG and DTA methods, it was established that 80% AlN–20% SiC powders start to oxidize in air at 830°C (Fig. 1) while 50% AlN–50% SiC powders start to oxidize at a temperature higher than 1000°C (Fig. 2). Oxidation of the 80–20 powders proceeds through three stages. Herein the maximum temperature for the first peak is 1105°C and, correspondingly, 1210°C for the second and 1347°C for the third stage (Fig. 1). If at the first and second stages only 4% of powder oxidizes then at the third stage (up to 1500°C) 7% oxidizes. It was ascertained by XRD and chemical analysis methods that the scale formed in the temperature range of 830–1170°C contains $Al_{10}N_8O_2$ aluminium oxynitride and also β-SiO_2 cristobalite. These interaction products form in accordance with thermodynamic predictions considering initial oxidation of components.

$$AlN + \frac{1}{10}O_2 = \frac{1}{10}Al_{10}N_8O_2 + \frac{1}{10}N_2 \qquad (1)$$

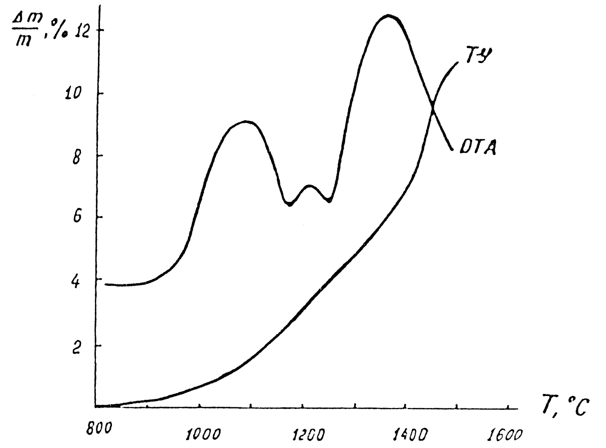

Fig. 1. TG- and DTA-curves for 80% AlN–20% SiC powders oxidation.

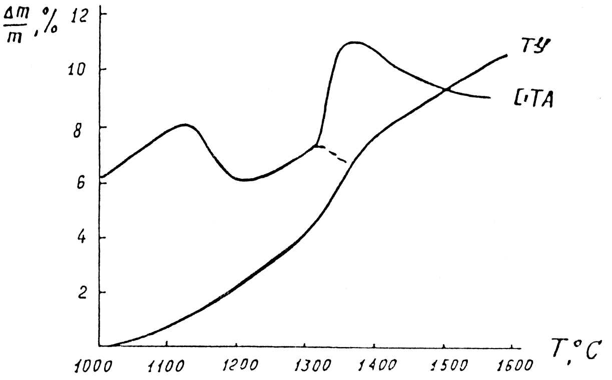

Fig. 2. TG- and DTA-curves for 50% AlN–50% SiC powders oxidation.

$$SiC + \frac{3}{2}O_2 = SiO_2 + CO \qquad (2)$$

In the temperature range of 1170–1250°C, during continued powder oxidation, a small amount of β-SiAlON forms. The sialon formation occurs as a result of the oxidation of SiC–AlN solid solution,[7] the latter being present in the initial heterophasic mixture in some quantity:

$$\begin{aligned}&[(SiC_{1-x})(AlN)_x] \xrightarrow{O_2} Si_{6-z}Al_zO_zN_{8-z} \\ &+ SiO_2 + CO + N_2\end{aligned} \qquad (3)$$

where $z = 4$.

At 1250–1500°C, mullite ($3Al_2O_3.2SiO_2$) is observed as a main phase of the oxide layer. Apparently, mullite formation is due mainly to the reaction:

$$\begin{aligned}&\frac{6}{10}Al_{10}N_8O_2 + 2SiO_2 \\ &+ \frac{39}{10}O_2 = 3Al_2O_3.2SiO_2 + \frac{24}{10}N_2\end{aligned} \qquad (4)$$

The more corrosion-resistant 50% AlN–50% SiC powder begins to oxidize at 1000°C. At 1100°C, its mass gain is equal to 0·6%. The oxidation maxima, as characterized by DTA occur at 1114 and 1353°C. At these maxima, the formation of oxidation products, i.e. $Al_{10}N_8O_2$ and β-SiO_2 for the first peak and $3Al_2O_3.2SiO_2$ for the third peak were observed. The second (intermediate) peak (Fig. 2) in this case is displaced to the higher temperature. The temperature of the second peak's maximum is 1300°C. By XRD, it was ascertained that unlike for the 80% AlN–20% SiC powder where at the second stage a small quantity of β-sialon forms, the 50% AlN–50% SiC forms α-Al_2O_3 from the oxynitride, according to the reaction:

$$Al_{10}N_8O_2 + 7O_2 = 5Al_2O_3 + 4N_2 + \frac{1}{2}O_2 \qquad (5)$$

In the same temperature range, β-cristobalite was also found in the scale.

For the third oxidation stage of 50% AlN–50% SiC powder, XRD and chemical analysis confirm the presence of $3Al_2O_3.2SiO_2$ and β-cristobalite in the surface scales formed at 1500°C. However, the appropriate interaction mechanism, in this case, differs from that of powder with 20% SiC and can be described by the reaction:

$$3Al_2O_3 + 2SiO_2 = 3Al_2O_3.2SiO_2 \qquad (6)$$

According to the TG-curves of Fig. 3, the compact AlN-SiC ceramics begin to oxidize at 1120°C, and the oxidation occurs in two stages. Herein the mass gain of 80% AlN + 20% SiC samples is significantly more, 0·37 mg/cm^2 for the first oxidation stage (up

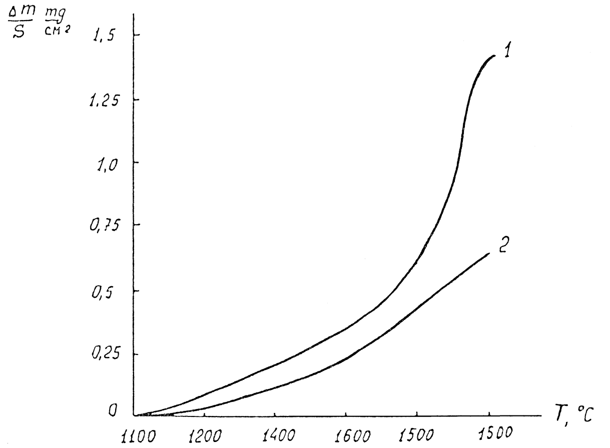

Fig. 3. Non-isothermal oxidation of AlN–SiC ceramics samples: 1. 80% AlN–20% SiC; 2·50% AlN–50% SiC.

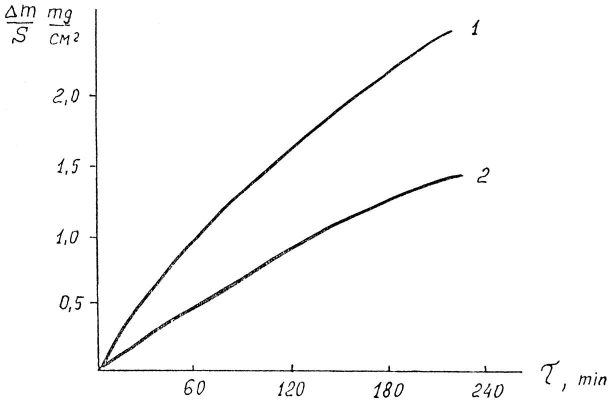

Fig. 4. Oxidation kinetics of (1) 80% AlN–20% SiC and (2) 50% AlN–50% SiC ceramics at 1350°C.

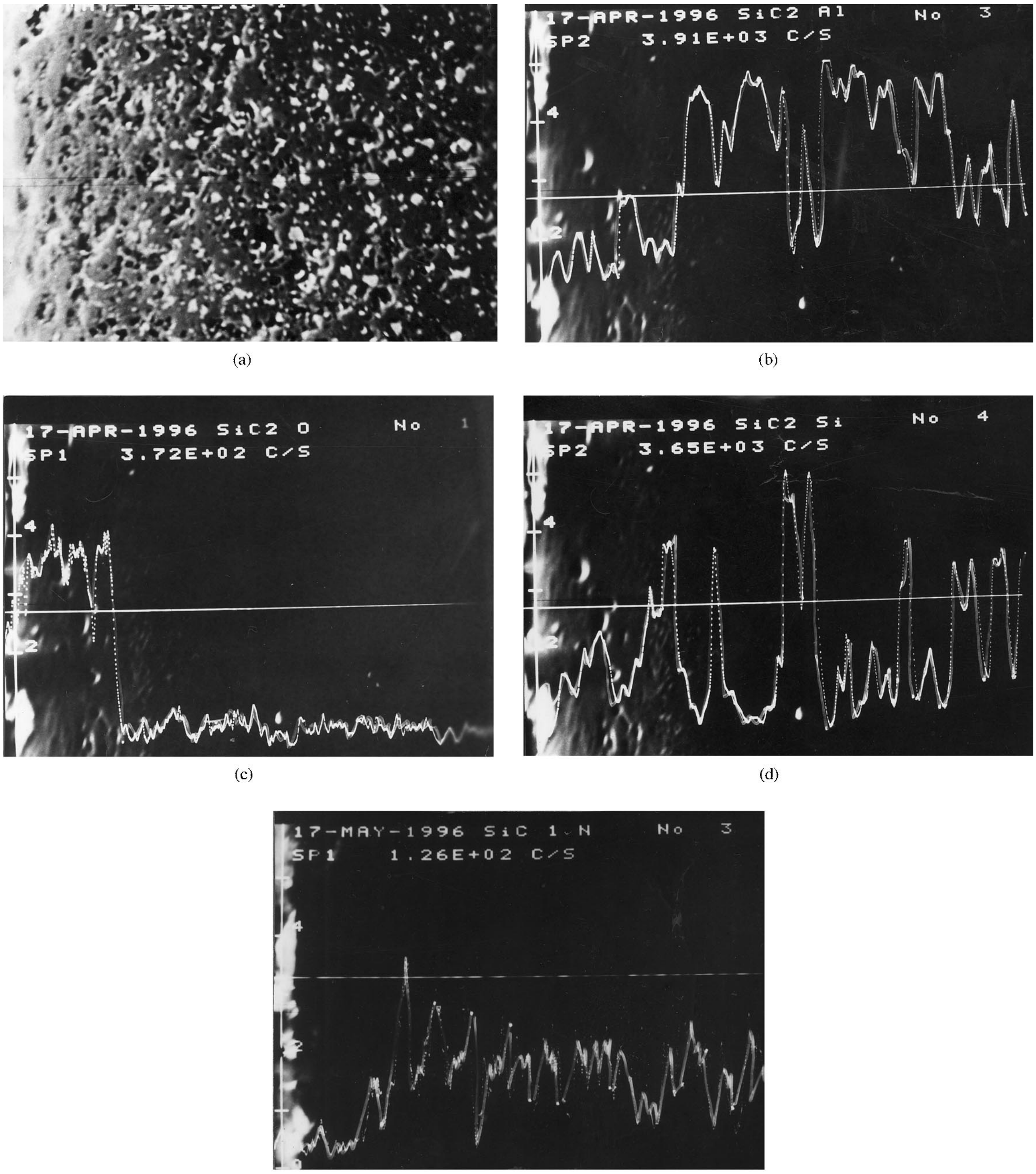

(a) (b)

(c) (d)

(e)

Fig. 5. Structure (a) and element distributions: (b) –Al; (c) –Si, (d) –O, (e) –N through the cross-section of the scale formed at high-temperature on 80% AlN–20% SiC ceramics up to 1550°C.

to 1440°C) and 1·42 mg/cm^2 for the second stage (up to 1560°C) than the samples with 50% SiC (0·25 and 0·65 mg/cm^2, respectively). However, both materials studied are extremely corrosion-resistant.

For the ceramics with 20% SiC, the first oxidation stage can be described by successive reactions (1), (2)→(3) while the second can be described by reaction (4). For the ceramics with greater SiC content, the first stage corresponds to reactions (1), (2)→(5) and the second stage to reaction (6). In Fig. 4, one can see the oxidation kinetics of compact ceramics at 1350°C. Their shape is not truly parabolic and a tentative determination of the parabolic rate constants shows that their value decreases with time (K$_1$, 60–80 min; K$_2$, 225 min):

$$80\%\ \mathrm{AlN} - 20\%\ \mathrm{SiC} \qquad K_1 = 2{\cdot}9 \times 10^{-10},\ K_2 = 1{\cdot}2 \times 10^{-10}\,\mathrm{g}^2\,\mathrm{cm}^{-4}\,\mathrm{s}^{-1},$$

$$50\%\ \mathrm{AlN} - 50\%\ \mathrm{SiC} \qquad K_1 = 1{\cdot}5 \times 10^{-10},\ K_2 = 0{\cdot}9 \times 10^{-10}\,\mathrm{g}^2\,\mathrm{cm}^{-4\ -1}$$

Such a behaviour confirms the evolutive nature of the oxide scale and consequently of its transport properties.

The EPMA and SEM data concerning element distributions and the morphologies of scale formed as a result of gradual heating and isothermal oxidation at temperatures up to 1550°C are shown in Fig. 5.

The dense scale formed on the 80% AlN + 20% SiC ceramics is characterized by a heterophasic structure (Fig. 5).

The structure can be divided into two zones. In the outer zone, the aluminium content is significantly more than that of silicon. In this zone, oxygen is present, but nitrogen is practically absent. According to XRD data, this is a mullite phase. In the inner layer β-SiO$_2$, Al$_{10}$N$_8$O$_2$ and β-sialon are observed. The oxygen and nitrogen contents are almost identical, while the aluminium content is two times more than that of silicon. The thickness of outer and inner layers is approximately the same and equal to 17–18 μm.

The scale formed on the 50% AlN + 50% SiC ceramics at the same temperatures and exposure times is characterized by extremely high adhesion to the material substrate. Its total thickness (17 μm) is only half that for the 80% AlN–20% SiC ceramics. According to EPMA data, only Al, Si and O were identified corresponding to a phase composition of $3\mathrm{Al_2O_3.2SiO_2} + \beta\text{-}\mathrm{SiO_2}$. XRD analysis failed to show the presence of the Al$_{10}$N$_8$O$_2$, β-sialon and α-Al$_2$O$_3$ phases.

4 Conclusion

1. The composition and structure of AlN-SiC ceramics as well as the oxidation conditions (air, 800–1550°C) exert a strong influence upon the kinetics and mechanism of scale formation and also the composition of interaction products. At short times of exposure in air and at comparatively low temperatures, β-cristobalite and aluminium oxynitride proved to be the main oxidation products, while at longer oxidation and higher temperatures (1350–1550°C), 3Al$_2$O$_3$.2SiO$_2$ (mullite) is the main interaction product.
2. β-sialon, present as an intermediate oxidation product in the inner scale layer, only in the case of 80% AlN–20% SiC ceramics, is formed, not due to oxidation of individual components (namely, AlN and SiC) but because of oxidation of a solid solution of SiC in AlN, which exists in the initial material.
3. High-temperature oxidation of 80% AlN–20% SiC and 50% AlN–50% SiC powders is defined by a three-stage oxidation regime revealed by the presence of three peaks on DTA-curves. The reaction mechanisms of the first and third stages are similar for different ceramic compositions and connected with β-SiO$_2$ and Al$_{10}$N$_8$O$_2$ formation for the first oxidation stage and 3Al$_2$O$_3$.2SiO$_2$ mullite for the third stage. The intermediate (second) peak on the DTA-curve for the 80% AlN–20% SiC powders corresponds to partial formation of β-sialon, while in the case of the 50% AlN–50% SiC powders, α-Al$_2$O$_3$ is formed.
4. The AlN–SiC ceramics studied, especially 50% AlN–50% SiC, proved to be exceptionally corrosion-resistant in air up to 1550°C, mainly, on account of mullite formation in the outer layer of the surface oxide film.

Acknowledgement

This research was supported by INTAS grant 94-1291.

References

1. Costello, J. A. and Tressler, R. E., Oxidation kinetics of silicon carbide crystals and ceramics: I, in dry oxygen. *J. Am. Ceram. Soc.*, 1986, **69**, 674–681.
2. Costello, J. A. and Tressler, R. E., Oxidation kinetics of hot-pressed and sintered SiC. *J. Am. Ceram. Soc.*, 1981, **64**, 327–331.
3. Heuer, A. H., Ogbuji, L. U. and Mitchell, T. E., The microstructure of oxide scales on oxidized Si and SiC single crystals. *J. Am. Ceram. Soc.*, 1980, **63**, 354–355.

4. Lavrenko, V. A. and Alexeev, A. F., Oxidation of sintered aluminium nitride. *Ceram. Int.*, 1983, **9**, 80–82.
5. Katnani, A. D. and Papathomas, K. I., Kinetics and initial stages of oxidation of aluminium nitride: thermogravimetric analysis and X-ray photo-electron spectroscopy study. *J. Vac. Sci. Technol.*, 1987, **A5**, 1335–1340.
6. Suryanarayana, D., Oxidation kinetics of aluminium nitride. *J. Am. Ceram. Soc.*, 1990, **73**, 1108–1110.
7. Xu, Y. and Zangvil, A., Formation of a β-sialon as an intermediate oxidation product of SiC–AlN ceramics. *J. Am. Ceram. Soc.*, 1995, **78**, 2753–2762.